Lead Zirconium Titanate Alternatives for Nanoactuators

Jin Wang, Gabe Elghoul, and Stephen Peters

***Abstract*—This paper describes the use of commercially available ceramic capacitors as an alternative for lead-containing and relatively expensive lead zirconate titanate (PZT)-based nanoactuators. A PZT actuator is compared with actuators made from both X5R- and Y5V-type ceramic dielectric capacitors using white light interferometry and a spectrometer. This work is useful because these capacitors can provide an economical nanomotion capability to research laboratories or industrial products. Measuring the displacement of the capacitors is also useful when designing electronic products to ensure undesired operation is not caused by the piezoelectric motion. Additionally, unlike the PZT material, the alternative ceramic materials do not contain lead, which is needed for full compliance with the Restriction on Hazardous Substances (RoHS) initiative.**

I. Introduction

Research into alternatives to the piezoelectric lead zirconate titanate (PZT)-type ceramic material is of interest for existing and future devices that move on the scale of nanometers. Some applications that could benefit from using alternative piezoelectric materials include ink jet printer heads [1], precision rotational stages [2], manipulating living cellular organisms [3], positioning semiconductor integrated circuits to align photo mask layers [4], research into new flexure stage control systems [5], and deformable mirrors for femtosecond laser pulse shaping [6]. Additionally, by determining the piezoelectric motion of commercial-grade capacitors, their use in electronic devices as capacitors can be better understood to avoid undesired operation. White light interferometry was chosen to measure the piezoelectric devices' change in length for this investigation because it has the ability to sense absolute distance [7] and the direction of motion. The signal-to-noise ratio can also be improved by averaging the intensity variations of multiple wavelengths, because all of the wavelengths see the same displacement. Each wavelength is measured by a different set of CMOS photodetectors and will have different electronic noise which can be averaged out over all of the different detectors.

II. Overall Setup

The overall setup of the experimental apparatus is depicted in Fig. 1. The source of the white light photons is an incandescent light bulb. A 650-nm, 5-mW laser diode is used for aligning the interferometer. The white light is passed through a lens and two irises to both collimate and control the intensity of the light going through the interferometer and the intensity of light coupled into the spectrometer. The interferometer is a Mach–Zehnder type made up of two nonpolarizing beam splitter cubes and two mirrors, as shown in Fig. 2.

III. Interferometer Setup

To align the interferometer to equal arm lengths, the method used by Colgate University was adapted with a few modifications [8]. One modification of the alignment technique is to use an adjustable Galilean beam expander to focus the alignment laser to either near or three meters away from the output of the interferometer. The alignment procedure then consists of using the beam expander to focus the alignment laser to spots just after the interferometer onto the temporary screen TS1, and translating BS1 until the spots overlap. Then the beam expander is adjusted to focus the alignment laser to spots on the viewing screen V1 three meters distant and make them overlap by adjusting the angle of the mirrors or BS2. Once the spots are aligned at both the near and far locations, the interferometer path length difference between the arms is small enough to optimize with the white light source and spectrometer.

The white light source shown in Fig. 3 consists of a light bulb mounted to a kinematic prism stage and a lens mounted on a cage rail system used to collimate the light from the bulb filament. The kinematic prism stage allows controlling the location of the filament with high precision in two dimensions for alignment purposes. An adjustable power supply is used to control the filament temperature and the spectrum of the white light. The lens and filament are positioned such that the alignment laser is centered on the lens and the alignment laser focuses to a spot on the filament. Light output from the interferometer is coupled to the spectrometer's SMA fiber using a lens and an SMA-to-SM1 adapter, as shown in Fig. 4.

The first step in setting up the white light interferometer is to make the two arm lengths close enough to identical path length to see white light fringes using a high-resolution spectrometer. The greater the arm length difference in the interferometer is, the higher is the modulation frequency of the spectrum as a function of wavelength. At a zero path length difference, the white light interferometer modulates all the wavelengths of light at once as the path

Manuscript received May 21, 2012; accepted October 14, 2012. Support for this research was provided by the University of Michigan Office of the Vice President for Research and the Rackham Foundation.

The authors are with the Department of Natural Science, University of Michigan, Dearborn, MI (e-mail: jinwang@umd.umich.edu).

DOI http://dx.doi.org/10.1109/TUFFC.2013.2556

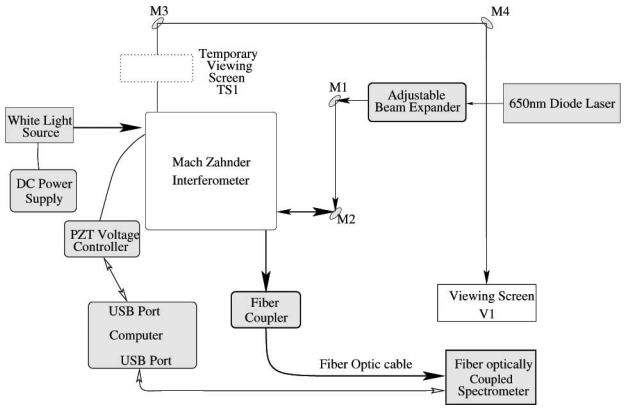

Fig. 1. The overall layout of the experimental apparatus. The source of white light is an incandescent flashlight bulb (T425). The light bulb's black body spectrum is modified by the Mach–Zehnder interferometer depending on the interferometer's relative arm lengths. The spectrometer measures the light spectrum and the spectra are recorded by the computer as the voltage on the piezoelectric material is varied.

length difference is changed. The spectrometer used in this experiment had a spectral resolution of around 2 nm, which worked well for both adjustment of the path lengths and acquiring the spectral data. Once the white light pattern is found, the relative arm lengths are adjusted using the spectrometer to minimize the modulation frequency of the spectrum. The setup of the white light interferometer also requires making the path length of the light traversing both arms the same for all wavelengths. The N-BK7 glass used in the cube beam splitters has different indices of refraction for different wavelengths. Therefore, the optical path lengths will only be the same for all frequencies of light if the light travels through the same amount of glass in each arm. To equalize the path length difference in the beam splitters for transmitted versus reflected light, the rotation angle of beam splitter BS2 or BS1 is adjusted to maximize the fringe visibility over all wavelengths detected by the spectrometer.

Because displacement on the scale of nanometers is detectable with this setup, all vibration sources in and even outside of the lab should be minimized. As the voltage on the piezoelectric devices is increased, the length of arm 2 in Fig. 2 becomes smaller as the material expands and pushes the stage holding BS1 toward mirror M1.

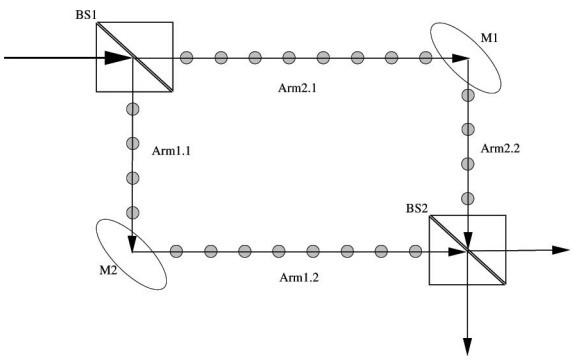

Fig. 2. The Mach–Zehnder interferometer used to determine the amount of movement in the piezoelectric material. The beam splitter BS1 translates to the right when the piezoelectric material expands.

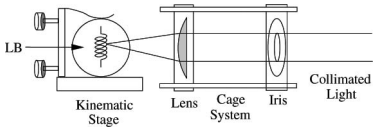

Fig. 3. The white light source setup. The incandescent light bulb LB is mounted to a kinematic prism stage such that its position can be moved in two dimensions for alignment purposes. The distance from the lens to the filament is adjusted by using a cage system and the diameter of the collimated light is adjusted by the iris.

IV. Experimental Setup

Nanoactuators were created out of individual X5R (C5750X5R1H106K, TDK Corp., Tokyo, Japan) and Y5V (C5750Y5V1C107Z, TDK Corp.) capacitors. Although the exact chemical composition of the X5R and Y5V capacitors is proprietary, according to the general capacitor manufacturer specification, both are predominantly barium titanate [9]. To create a material thickness out of the 2.3-mm-thick capacitor-based devices comparable to the 5-mm PZT, two Y5V ceramic capacitors were stacked on top of each other for a total Y5V material thickness of 4.6 mm. The X5R assembly consisted of three capacitors with two glass separators and glass on the ends, giving a total X5R material length of 6.9 mm. The Y5V capacitor assembly is shown in Fig. 5. The PZT actuator (AE-0203D04F, NEC Token, Tokyo, Japan) is 5 mm long and is made of N-10 material [10]. The purchase prices for each X5R, Y5V, and PZT device were \$1.87, \$1.84, and \$72.80 respectively.

The glass was used between the capacitors to ensure that the capacitors were only contacting each other on their active ceramic areas, avoiding the metal bonding pads on the ends. The reason for this is that the piezoelectric material near the electrodes does not experience as much electric field as the middle of the capacitor, where the material experiences the full electric field. The glass on the outer part of the assemblies also provides a smooth surface for the micrometer screw head to turn, allowing coarse adjustment of the location of BS1.

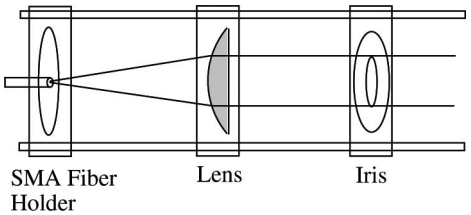

Fig. 4. The spectrum analyzer fiber coupler setup showing the light from the interferometer entering from the right. The light travels through the iris which controls the intensity of the light reaching the spectrometer. The light is then focused by the lens into the optical fiber attached to the spectrometer.

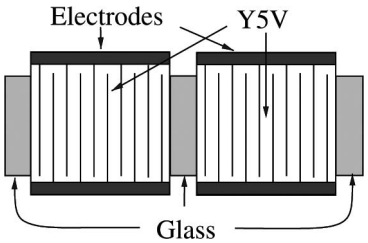

Fig. 5. The assembly used to measure the piezoelectric expansion caused by an applied voltage on the Y5V capacitors.

Because of the size differences between the samples, the interferometer must be realigned using the guide laser and the procedure in the previous section. Before collecting data for each piezoelectric device, the visibility of the white light interference pattern is optimized. Additionally arm 2 is made shorter than the equal path length to modulate the spectrum to get around ten peaks. The direction of the fringe pattern shift verses wavelength allows determination of whether the piezoelectric is expanding or contracting. Voltage is applied to the piezoelectric device under test by a TPZ001 piezo controller (Thorlabs Inc., Newton, NJ). The controller is capable of supplying a voltage between 0 and 150 V to the piezoelectric devices. The piezoelectric samples are placed between the end of a micrometer and the moving part of the translational stage holding the beam splitter BS1, as shown in Fig. 6.

V. Experimental Results

For the experimental collection of data, the maximum voltage range of each piezoelectric element was split into 200 steps. The spectral data range taken for each voltage was from 200 to 1024 nm using a CCS200 spectrometer (Thorlabs Inc.) with a spectral error of less than 2 nm. Samples of the spectral data for each applied voltage were collected every 20 ms, and then averaged over 2.5 s. To visualize the experimental data, a two-dimensional image of the results for the Y5V-type capacitor is shown in Fig. 7. In the figure, the voltage changes vertically and the wavelengths vary horizontally. The average spectral intensity at each voltage step and each wavelength is color coded. The slope of the peak spectral wavelengths as the voltage is varied indicate the material expands as the voltage increases up to 16 V and contracts as the voltage decreases back to zero. In comparing all three devices the applied voltage is normalized to the maximum voltage tested for each device. Fig. 8 shows a plot of the intensity of 492.7 nm

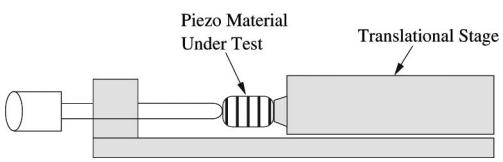

Fig. 6. Side view of the location of the piezoelectric material under test in the linear translator holding BS1.

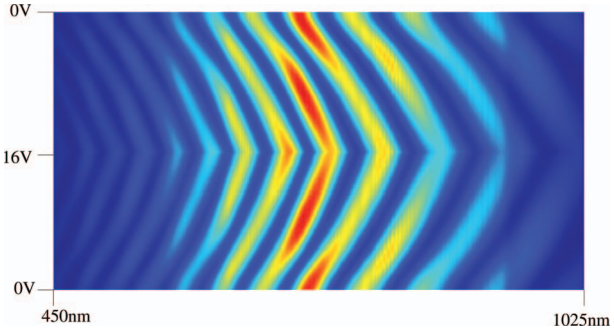

Fig. 7. Spectral intensity data taken for the Y5V capacitor at different voltages. At the top of the figure, the voltage is zero; for each row going down, the voltage is increased by 0.08 V until reaching 16.0 V in the middle. From the middle to the bottom, the voltage decreases from 16 V to 0 V in 0.08 V steps. The amplitude is encoded into color such that blue represents the lowest intensity and red the highest intensity.

as the Y5V, X5R, and PZT element voltages are varied from 0 to the normalized maximum device voltage. As can be seen from the number of fringes that pass for each type of material, the PZT material undergoes the most displacement over its entire voltage range compared with the other two materials. The actual displacement of the capacitor is measured by converting the fringe intensity pattern to a phase angle. The fringe intensity graphs were converted to a phase angle by finding the best quadratic phase coefficients of (1) to fit the experimental data:

$$I(V) = I_m \sin(\alpha V^2 + \beta V + \gamma) + I_0, \tag{1}$$

where I_m is the intensity of the interference pattern; I_0 is the average intensity; and α, β, and γ are the quadratic coefficients that were found to best approximate the experimental data. The next step in finding the displacement is to note that for the Mach–Zehnder interferometer, a 2π change of phase angle is equivalent to one wavelength λ of displacement. The displacement is thus obtained by multiplying the quadratic estimate of the phase by $\lambda/2\pi$. Because of the different lengths of material, the displacements of the Y5V and X5R capacitors were scaled by 1.09 and 0.72 respectively. The results of converting the displacement over each device's normalized voltage operating range are plotted in Fig. 9.

The final result shown in Fig. 10 is that the two commercial-capacitor-based piezoelectric elements (X5R and Y5V) both have a higher displacement per volt compared with the PZT material. The maximum displacement of each actuator is 278.3, 381.9, and 843.3 ppm. The displacement of the Y5V, X5R, and PZT are 17.4, 7.64, and 6.02 ppm/V. The PZT actuator has a manufacturer-specified displacement of 4.6 ± 1.5 μm at 150 V and a length of 5 mm. The PZT actuator is specified to have a 6.1 ± 2 ppm change in length per volt, which agrees with the experimental results. For the total displacement per unit length, the X5R material yields approximately 50% of the displacement of PZT. However, the X5R only requires 33% of the maximum PZT voltage, which may make it

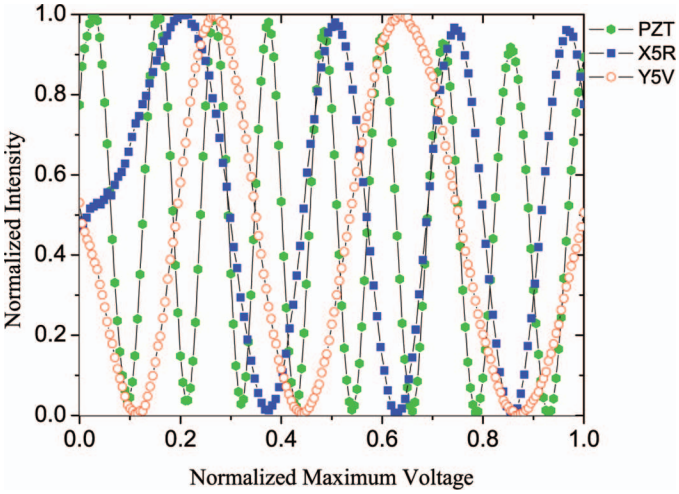

Fig. 8. Comparison of the interference patterns generated by PZT, Y5V, and X5R at a wavelength of 492.7 nm. The x-axis has been scaled such that 0 corresponds to 0 V, and 1 corresponds to the maximum voltage for each material type.

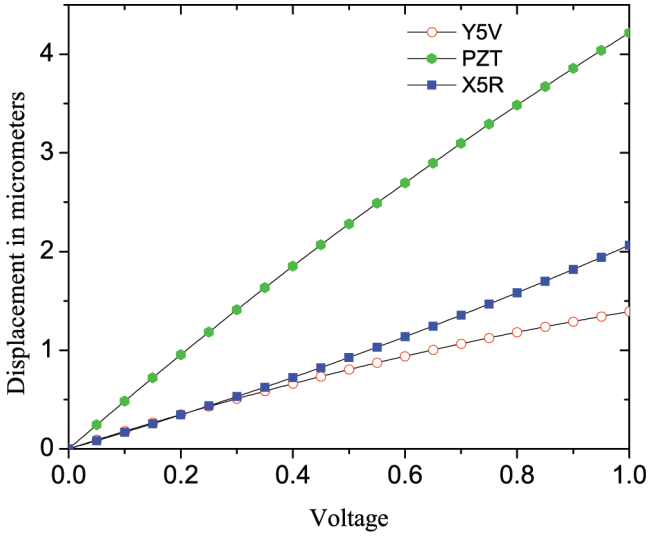

Fig. 9. This figure compares the displacement generated by PZT, Y5V, and X5R as measured at a wavelength of 492.7 nm. The x-axis has been scaled such that 0 corresponds to 0 V, and 1 corresponds to the maximum voltage for each material type. From top to bottom, the lines represent PZT, X5R, and Y5V, respectively.

suitable for lower voltage applications. For the Y5V material, the total displacement per unit length was about 37.5% of the PZT material. For applications requiring an even lower voltage and higher displacement per volt, the Y5V material may be the best choice with the lowest maximum voltage (11% of the voltage that the PZT material requires) and the highest displacement per volt rating. Additionally, this material is an order of magnitude less expensive than PZT.

VI. Discussion and Summary

Another similar technique for measuring the displacement of a piezoelectric sample at a high rate of motion is to use a Fabry–Perot etalon interferometer made from the end of an optical fiber and a piezoelectric sample coated with a mirror surface [11]. The etalon technique also uses white light (with a full-width at half-maximum bandwidth of 30 nm) but requires a mirror surface to be added to the piezoelectric material, which would add significantly to the cost.

Some theoretical background and experimental results of the interferometer experiments are discussed subsequently. Intuitively, one could assume that when voltage is applied to the capacitors, they should get smaller because the plates have opposite charges and will be attracted to each other. However, when voltage is applied to piezoelectric materials, they actually expand. Piezoelectric materials such as PZT derive their piezoelectric capability from their underlying crystal structure, which naturally creates a stable electric dipole below the Curie temperature. When an electric field is applied to the material, the dipoles align with the field and cause the material to expand. The piezoelectric expansion is opposite to the force of attraction between the plates resulting from the positively and negatively charged plates.

To expand and contract with maximum displacement in the piezoelectric material, the effective capacitance of the material must be charged and discharged. The capacitance of the PZT material is 0.09 μF ± 20%. The energy to required to fully charge the PZT is 0.98 ± .20 mJ. The X5R and Y5V capacitors are 10 ± 10% μF and 100 + 80%, − 20% μF respectively. The energy required to fully charge the X5R and Y5V capacitors is 25 ± 2.5 mJ and from 20 to 45 mJ respectively. The X5R and Y5V materials' higher capacitance requires 25 times the energy to fully expand from its initial state, but this energy is very manageable at 25 mJ if the device is used as a static positioning device. The higher capacitance value of the Y5V and X5R devices can also help stabilize the voltage across

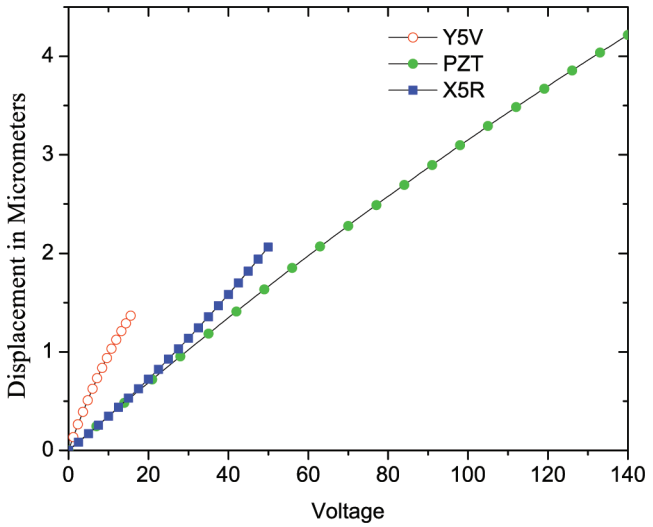

Fig. 10. The displacement per unit volt of Y5V, X5R, and PZT. From top to bottom, the lines represent Y5V, X5R, and PZT, respectively.

their electrodes, which is useful in an electromagnetically noisy environment. One practical advantage of the X5R and Y5V capacitors over PZT is that they can be operated in forward or reverse polarity without damage, unlike PZT, which is damaged if operated in reverse polarity greater than the coercive field.

Overall, the X5R and Y5V-type capacitors are good alternatives to the traditional PZT nanoactuators, because of their lower voltage requirements, order of magnitude lower cost, significant relative expansion (50% and 37%, respectively) compared with that of a PZT actuator, insensitivity to polarity, and because they do not contain any lead.

Acknowledgments

J. Wang acknowledges support and valuable discussions with D. Bord, J. Prentis, and V. Naik.

References

[1] K.-S. Kwon, Y.-S. Choi, D.-Y. Lee, J.-S. Kim, and D.-S. Kim, "Low-cost and high speed monitoring system for a multi-nozzle piezo inkjet head," *Sens. Actuators A*, vol. 180, pp. 154–165, Jun. 2012.

[2] H. Zhu and A. Asundi, "Characterization of piezo rotation stage by multipoint diffraction strain sensor," *Phys. Proc.*, vol. 19, pp. 173–177, 2011.

[3] F. Imura, F. Nakada, Y. Egashira, H. Kubota, K. Kosaka, T. Kosaka, H. Kagami, K. Masuda, J. Hamada, M. Tada, and T. Moriuchi, "Development of nano-surgery system for cell organelles," in *Proc. 41st SICE Annu. Conf.*, 2002, vol. 5, pp. 3236–3241.

[4] I. A. Ivan, M. Rakotondrabe, J. Agnus, R. Bourquin, N. Chaillet, P. Lutz, J.-C. Poncot, R. Duffait, and O. Bauer, "Comparative material study between PZT ceramic and newer crystalline PMN-Pt and PZN-Pt materials for composite bimorph actuators," *Rev. Adv. Mater. Sci.*, vol. 24, no. 1/2, pp. 1–9, 2010.

[5] H. C. Liaw, B. Shirinzadeh, and J. Smith, "Robust motion tracking control of piezo-driven flexure-based four-bar mechanism for micro/nano manipulation," *Mechatronics*, vol. 18, no. 2, pp. 111–120, 2008.

[6] C. Radzewicz, P. Wasylczyk, W. Wasilewski, and J. S. Krasiski, "Piezo-driven deformable mirror for femtosecond pulse shaping," *Opt. Lett.*, vol. 29, no. 2, pp. 177–179, 2004.

[7] L. M. Manojlovic, "A simple white-light fiber-optic interferometric sensing system for absolute position measurement," *Opt. Lasers Eng.*, vol. 48, no. 4, pp. 486–490, 2010.

[8] E. Galvez. (2010, Mar.) Correlated-photon experiments for undergraduate labs, [Online]. Available: http://departments.colgate.edu/physics/research/Photon/Photon%20research/Quantumlan07/Lab%20Manual2010.pdf

[9] TDK Corp. (2009, Mar.) Specification for TDK multilayer ceramic chip capacitors. [Online]. Available: http://www.tdk.com/pdf/cap_general_spec_standard.pdf

[10] NEC-Tokin Corp. (2010, Mar.) Piezoelectric ceramics. [Online]. Available: http://www.nec-tokin.com/english/product/pdf_dl/piezoelectricceramics.pdf

[11] R. E. da Silva, R. A. Oliveira, and A. A. P. Pohl, "Fiber Fabry-Perot interferometer sensor for measuring resonances of piezoelectric elements," *Proc. SPIE*, vol. 7753, art. no. 775319, 2011.

Jin Wang was born in Yangzhou, China. She received her Ph.D. degree in physics from the University of Queensland, Australia, in 2001. She is currently an assistant professor of physics in the University of Michigan–Dearborn, and a member of the American Physical Society (APS). Dr. Wang's research focus is on quantum optical phenomena.

Gabe Elghoul is an undergraduate student at the University of Michigan–Dearborn, majoring in biology. Gabe takes special interest in quantum theory, web programming, and medical science.

Stephen Peters is an undergraduate student at the University of Michigan majoring in physics and mechanical engineering. Peter has a special interest in aerospace engineering.